Inverse correlation between the intensity of luminescence excited by electrons and by visible light in chemical-vapor-deposited diamond films

L. H. Robins, E. N. Farabaugh, A. Feldman, and L. P. Cook
National Institute of Standards and Technology, Ceramics Division, Gaithersburg, Maryland 20899
(Received 22 October 1990)

Diamond films grown by filament-assisted or microwave-plasma-assisted chemical-vapor deposition (CVD) were characterized by photoluminescence (PL), cathodoluminescence (CL), and Raman spectroscopies. The laser-excited PL spectra of these films in and near the carbon Raman region (1100–1800 cm^{-1} from the 514.5-nm laser line, or 2.18–2.28 eV) are broad and featureless; CL spectra measured within a wider spectral range (1.5–3.5 eV) show several distinct components. Because of its correlation with the Raman band of sp^2-bonded carbon, the visible-laser-excited PL in the carbon Raman region is attributed to sp^2-bonded carbon clusters. The spectrally integrated CL intensity is found to vary from specimen to specimen approximately inversely with the intensity of the laser-excited PL. This inverse correlation is especially strong for one component of the CL, a broad band at 2.85 eV. To explain these results, it is proposed that the luminescence centers in these CVD diamond films can be classified into two types with differing excitation and recombination properties. Rate equations are derived for the luminescence kinetics of such a system of two types of recombination centers.

INTRODUCTION

Luminescence spectroscopy is increasingly recognized as one of the most sensitive probes of defects in chemical-vapor-deposited (CVD) synthetic diamond.[1,2] The luminescence of CVD diamond has been attributed to point defects, impurities, extended defects such as dislocations, and moleculelike complexes of two or more point defects and/or impurity atoms.[3] Most studies of luminescence in diamond have made use of excitation either by visible or ultraviolet light [photoluminescence (PL)] or by an electron beam [cathodoluminescence (CL)].

When CVD diamond specimens are excited by visible light, a broad, featureless PL band is generally observed. This PL begins at a photon energy close to that of the excitation, and extends throughout the carbon Raman region (1100–1800 cm^{-1} from the 514.5-nm laser line, or 2.18–2.28 eV). In Raman spectroscopy, this broad PL is often denoted the PL background or fluorescence background. We recently reported, based on a study[5] of the Raman spectra of 48 diamond specimens grown by filament-assisted or microwave-plasma-assisted CVD, that the intensity of the PL background is strongly correlated with the intensity of the sp^2-bonded carbon Raman band. The latter band peaks at a wave-number shift of $\sim$1525 cm^{-1} and has a full width at half maximum (FWHM) of $\sim$200 cm^{-1}. Because of this correlation, we suggested[5] that the PL background arises from clusters of sp^2-bonded carbon atoms within the mainly sp^3-bonded diamond films, similarly to the PL in amorphous hydrogenated carbon or in polynuclear aromatic molecules.

Here we present the results of a comparative study of the visible-excited PL, Raman, and CL spectra of the set of CVD diamond specimens characterized in the previous study.[5] For this set of specimens, the CL intensity is found to be *inversely* correlated with the intensity of the visible-excited PL background. This inverse correlation is particularly strong for one component of the CL, a broad band centered at 2.85 eV. A model of recombination at two types of luminescence centers with differing properties is proposed to explain the inverse correlation. In the context of this model, it is shown that recombination at the two types of centers may proceed either independently or competitively, depending on the nature of the excitation process.

EXPERIMENTAL PROCEDURE

Experimental details of the filament-assisted and microwave-plasma-assisted depositions have been presented elsewhere.[1,5] Conditions for a typical filament-assisted deposition were the following: gas mixture, 99.5% H_2, 0.5% CH_4; nominal substrate temperature, 750 °C; nominal filament temperature, 1800 °C; pressure, 5×10^3 Pa; gas flow rate, 50 standard cm^3/min (SCCM). Conditions for a typical microwave-plasma-assisted deposition were the following: gas mixture, same; nominal substrate temperature, 650 °C; microwave power, 1000 W; pressure, 7×10^3 Pa; gas flow rate, 260 SCCM. (The nominal substrate temperature is measured by a thermocouple connected to the substrate support; the actual temperature at the growth surface may be considerably higher.) Among the parameters varied from one deposition to another were substrate temperature, methane fraction, deposition time, and, in the filament-assisted depositions, filament geometry. In some depositions, oxygen was also added to the gas mixture; addition of a small amount of oxygen has been shown to reduce the nondiamond content of the films.

The PL (Ref. 5) and CL (Ref. 1) spectral measurements have also been discussed elsewhere. PL and Raman scattering were excited by an Ar^+ laser at 514.5 nm. The incident laser power was 80 mW, and the laser spot size was $\sim 100\ \mu$m. CL was excited by the electron beam of a scanning electron microscope; typically, the electron-beam voltage was 20 kV, the beam current was $\sim 10^{-8}$ A, and the beam was rastered over a 55×70-μm^2 area. The wavelength resolution of the laser PL and Raman spectra was 0.1 nm (0.4 meV, or 3 cm^{-1}, at 2.25 eV); the resolution of the CL spectra was considerably lower, 0.7 nm (3 meV at 2.25 eV). (High wavelength resolution was needed in order to determine the width of the narrow diamond Raman line.) For all spectra, the wavelength scale was calibrated with noble-gas atomic-vapor lamps. All spectra were normalized by dividing by the system optical response, which was determined with lamps of the same types used as National Institute of Standards and Technology (NIST) spectral irradiance standards.

EXPERIMENTAL RESULTS

Raman spectra of the 48 CVD diamond specimens were measured from 1100 to 1800 cm^{-1}, which is considered to be the carbon Raman region. The Raman spectra consist of two components: the crystalline diamond line at 1333 cm^{-1}, and the Raman band of disordered sp^2-bonded carbon, which peaks at ~ 1525 cm^{-1} and has a FWHM of ~ 200 cm^{-1}. As mentioned above, a broad, featureless PL background was observed together with the Raman spectrum of each specimen. Additional spectral measurements have shown that the PL band extends to at least 5000-cm^{-1} shift from the 514.5-nm laser line (i.e., to 1.8 eV) with little change in intensity.

Representative PL and Raman spectra of three specimens are plotted in Fig. 1. Of these three, the "best" Raman spectrum, labeled (i), with the narrowest diamond line and the least sp^2-bonded carbon band and PL background, was obtained for a microwave-plasma-assisted deposition under the following conditions: gas mixture 0.5% methane, 0.5% oxygen, 99% hydrogen: nominal substrate temperature 650 °C; deposition time 18 h. The other two spectra, labeled (ii) and (iii), were obtained for specimens grown in the bell jar filament-assisted reactor under the following conditions: gas mixture 0.5% methane, 99.5% hydrogen; nominal substrate temperature 750 °C; deposition time, 72 h. The dimensions of the hot filament differed for the latter two depositions, probably accounting for the differences in the Raman spectra. The three spectra of Fig. 1 typify the variation in Raman line shape for all specimens in the present study.

A model line-shape function, discussed in a previous publication,[5] was designed to numerically fit spectra like those shown in Fig. 1. It is desirable to fit the data in order to obtain numerical values for parameters such as the FWHM of the diamond Raman line or the intensity of the PL background relative to that of the diamond line. The model function is the sum of the following three components: a symmetric bell-shaped function defined as the product of a Lorentzian to the power β $(0 < \beta < 1)$ and a Gaussian, chosen to represent the diamond Raman line; a Gaussian function, chosen to represent the sp^2-bonded carbon Raman band; and a quadratic polynomial $(a + bx + cx^2)$, chosen to represent the PL background. The selected function has been shown to fit the data well, although other functions might also be designed for this task.

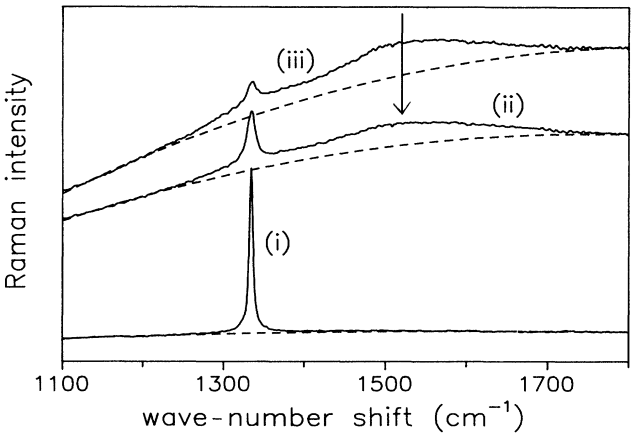

FIG. 1. Photoluminescence (PL) and Raman spectra of three CVD-grown diamond films, illustrating the range of line shapes observed for the 48 films examined in the present study. Spectra are multiplied by arbitrary scale factors to facilitate comparison in the same graph. The broad Raman band of sp^2-bonded carbon, centered at ~ 1525 cm^{-1}, is indicated by arrow. Fitted PL background functions (quadratic polynomials) are indicated by dashed lines underlying experimental spectra. Specific deposition conditions for films (i), (ii), and (iii) are given in text.

In Fig. 2, the specimen-to-specimen variation of the intensity of the PL background at 1450 cm^{-1} is compared with the variation of the peak intensity of the sp^2-bonded carbon Raman band; both intensities are given as ratios to the diamond Raman peak. The parameter values shown in Fig. 2 were obtained by fitting the data to the model function described above. Each CVD specimen is represented by a distinct data point in Fig. 2. For comparison, results for a gem-quality natural diamond, which shows a very weak PL background and no observable sp^2-bonded carbon band, are also plotted. It can be seen that there is a strong positive correlation between the intensity of the two parameters plotted in Fig. 2. A plot of the type shown in Fig. 2 can be used to determine whether any two spectral parameters are correlated.

Representative CL spectra in the 1.5–3.5-eV range of three specimens are plotted in Fig. 3. (These are not the same specimens chosen for Fig. 1; a different group of specimens was selected to best display the variation in behavior of the CL spectrum.) The CL spectra are seen to consist of several distinct components, which are indicated in Fig. 3. The centers that give rise to these components have ben tentatively identified by comparison with known luminescence centers in natural and synthetic gem-quality diamonds,[1,6] as follows: Component (a), the narrow line at 1.68 eV, is attributed either to a silicon

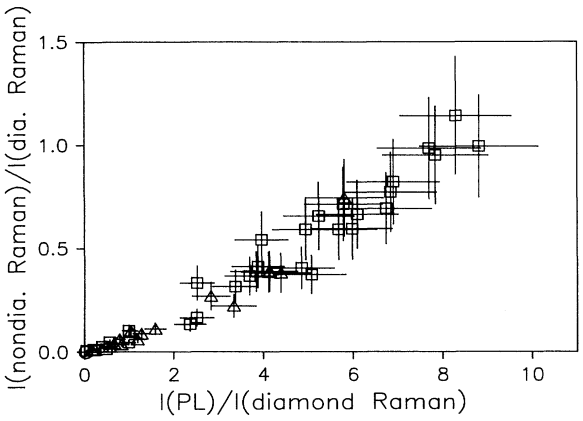

FIG. 2. Correlation between intensity of visible-excited PL (spectral background seen in Fig. 1) and peak intensity of sp^2-bonded carbon Raman band (ratios to diamond Raman peak). Each data point represents one specimen. Data are for 32 diamond films grown by filament-assisted CVD (squares), 16 films grown by microwave-plasma-assisted CVD (triangles), and one gem-quality natural diamond (circle).

impurity center,[7] which has its zero-phonon line at 1.684 eV, or to the single-atom vacancy [general radiation (GR) center],[3] which has its zero-phonon line at 1.673 eV. Component (b), the narrow line at 2.155 eV and phonon sidebands at lower energy (observed here as an unresolved broad band centered at ~2 eV), is attributed to a nitrogen-vacancy center composed of a single nitrogen atom and one or more vacancies.[8,9] Component (c), the narrow line at 2.325 eV, is also attributed to a nitrogen-vacancy center.[10] Component (e), the broad symmetric band centered at 2.85 eV, is tentatively attributed to deep donor-acceptor pairs; this band has been topographically correlated with dislocations in some natural diamonds.[11] We have retained the previous designation of components (a)–(e) for consistency.[6] Not shown in Fig. 3 is component (d), a narrow line at 3.188 eV with well-resolved phonon sidebands, attributed to a nitrogen-interstitial center.

More experimental work is needed to determine the sources of the nitrogen and silicon impurities associated with some of the observed CL centers, as described above, and to measure the absolute concentrations of these impurities. It is not difficult to find possible sources in our deposition process for trace levels of nitrogen or silicon. Nitrogen may originate from atmospheric contamination of the deposition system, or from trace contaminants in the source gases. The main source gas, high-purity hydrogen, contains up to 5 ppm N_2. Silicon substrates were used in most depositions. During a deposition on a silicon substrate, silicon may enter the film either by solid-state diffusion from the substrate or by sputtering from the substrate into the gas phase and subsequent incorporation. In the microwave-plasma reactor, another possible source of silicon is the fused-silica top window of the plasma-containing cavity.

The widths of the narrow CL lines referred to above as components (a), (b), and (c) were found to vary by a significant amount from specimen to specimen, and some variation of the peak positions was also observed. For component (a), the peak position varied from 1.675 to 1.680 eV and the FWHM varied from 13 to 23 meV; for component (b), the peak position varied from 2.147 to 2.156 eV and the FWHM varied from 15 to 40 meV; and for component (c), the peak position varied from 2.317 to 2.326 eV and the FWHM varied from 10 to 40 meV. We did not find any pair of parameters within this set of three peak positions and three linewidths to be significantly correlated; nor was there a significant correlation between any of these parameters and the Raman

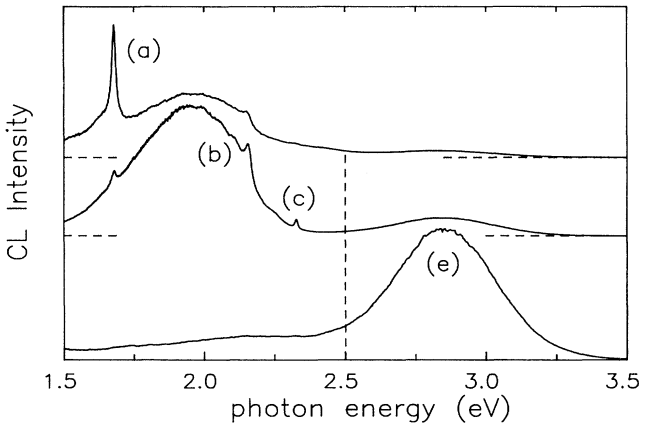

FIG. 3. Cathodoluminescence (CL) spectra of three CVD-grown diamond films. Spectra are offset for ease of comparison; horizontal dashed lines indicate baseline offsets. Vertical dashed line indicates division between 1.5–2.5- and 2.5–3.5-eV energy ranges, utilized in Fig. 5. Components (a), (b), (c), and (e) of CL spectra are discussed in text.

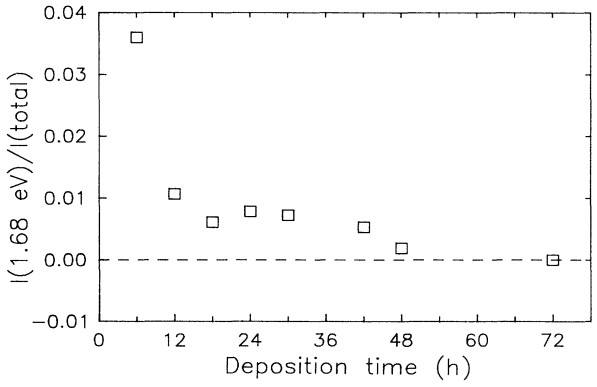

FIG. 4. Correlation between integrated intensity of 1.68-eV CL line, ratioed to total integrated CL intensity from 1.5 to 3.5 eV, and growth time. Data are for one set of filament-assisted CVD specimens deposited on silicon substrates from 0.5% methane in hydrogen at a nominal substrate temperature of 750 °C.

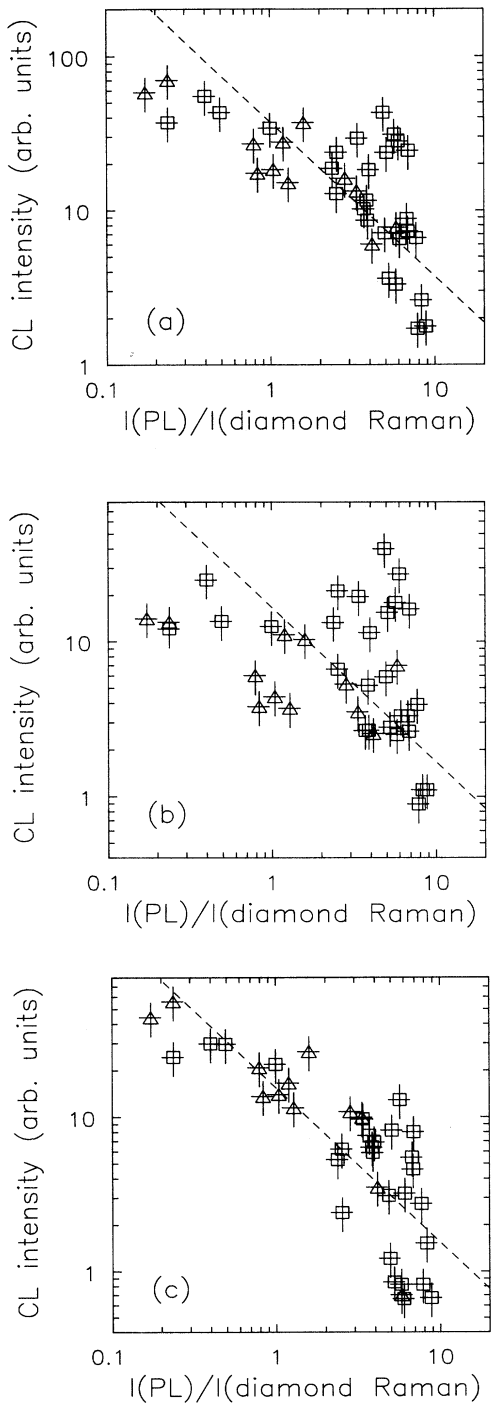

FIG. 5. (a) Correlation between visible-excited PL intensity (intensity ratio to diamond Raman peak, as shown in Fig. 2) and total CL intensity, spectrally integrated from 1.5 to 3.5 eV. (b) Correlation between intensity of visible-excited PL and of lower-photon-energy CL bands, spectrally integrated from 1.5 to 2.5 eV. (c) Correlation between intensity of visible-excited PL and of higher-photon-energy CL bands, spectrally integrated from 2.5 to 3.5 eV. In these plots, triangles represent filament-assisted depositions; squares represent microwave-plasma-assisted depositions. Dashed lines show best fits of data to simple inverse correlation ($I_{CL} \propto 1/I_{PL}$).

parameters discussed above.

The intensity of the 1.68-eV line [component (a)] was observed to be highest, relative to the other components of the CL, for specimens in which the average thickness of the diamond deposition was small; these included specimens consisting of unconnected particles. This behavior is shown in Fig. 4, where the ratio of the integrated intensity under the 1.68-eV peak to the total integrated CL intensity (from 1.5 to 3.5 eV) is plotted as a function of growth time for one set of filament-assisted depositions. The relative intensity of the 1.68-eV line is seen to decrease with increasing growth time. (Within this set, the specimen grown for 6 h consists of unconnected particles; the particles are partially connected at 12 h; and at 18 h and longer the specimens are continuous films.) These results suggest that formation of the 1.68-eV center is enhanced by close proximity to a silicon substrate. This observation supports the silicon impurity model for the 1.68-eV center.

The surprising inverse correlation between the CL intensity and the intensity of the PL background in the carbon Raman region is shown in Fig. 5. The independent parameter of Fig. 5 is the intensity ratio of the PL to the diamond Raman peak, as in Fig. 2. In Fig. 5(a), the dependent parameter is the total CL intensity (integrated from 1.5 to 3.5 eV); in Fig. 5(b), the dependent parameter is the intensity of the lower-photon-energy CL bands (integrated from 1.5 to 2.5 eV); and in Fig. 5(c), the dependent parameter is the intensity of the higher-photon-energy CL bands (integrated from 2.5 to 3.5 eV). Note that while some of the 48 CVD specimens contain unconnected particles, only data for continuous films are included in Fig. 5. Specimens that contain unconnected particles are excluded from Fig. 5 because incomplete coverage of the substrate by the diamond deposition reduces the observed CL intensity, and we do not know how to correct for this effect.

The CL integrated from 1.5 to 2.5 eV, shown in Fig. 5(b), arises primarily from spectral component (b) indicated in Fig. 3, together with components (a) and (c). The CL integrated from 2.5 to 3.5 eV, shown in Fig. 5(c), arises almost entirely from spectral component (e) of Fig. 3, the broad violet (2.85 eV) band. (Note that the division between the 1.5–2.5-eV and 2.5–3.5-eV energy ranges is marked in Fig. 3.) The inverse correlation between the PL and CL holds better for component (e), as indicated by Fig. 5(c), than for components (a), (b), and (c), as indicated by Fig. 5(b).

DISCUSSION

Let us first examine the reason for the correlation between the intensity of the sp^2-bonded carbon Raman band and the intensity of the PL background in the Raman region. For PL to be excited, the incident laser light (at 514.5 nm, or 2.41 eV) must be at least partially absorbed within the specimen. A perfect diamond crystal, free of all defects and impurities, is transparent to visible light; thus the absorption of the incident laser light in the CVD specimens must proceed through defects, impurities, or nondiamond carbon phases. Consider the defect

states or nondiamond phases that are composed of sp^2-bonded clusters of carbon atoms. Such a cluster may alternately be called a π-bonded cluster because of the associated π-bonded electron system. An sp^2-bonded (π-bonded) carbon cluster of intermediate size gives rise to optical absorption and to a broad PL band in the visible region. (The size of a cluster may be defined as the length of the longest sp^2-bonded chain in the cluster; clusters with a chain length of approximately six to ten atoms both absorb and emit visible light.) The optical absorption and PL attributed to sp^2-bonded carbon clusters have been observed in amorphous hydrogenated carbon films.[12] The correlation between the sp^2-bonded carbon Raman band and the broad visible-excited-and-emitted PL (i.e., the PL background in the Raman region) in CVD diamond films can thus be plausibly explained by the assumption that this type of PL arises from sp^2-bonded carbon clusters.

A model to explain the inverse correlation between the CL and the visible-excited PL, which is shown in Fig. 5, will now be proposed. We will first describe the model in qualitative terms, and then develop a set of rate equations in order to derive quantitative relations between various model parameters. The key assumptions of the model are as follows. Luminescence centers in these CVD diamond films can be classified into two general types. Centers of the first type have a high luminescence quantum efficiency and a small optical-absorption coefficient in the visible region; conversely, centers of the second type have a low luminescence quantum efficiency and a large optical absorption coefficient in the visible region. Centers of the first type give rise to all of the observed CL [components (a)–(e) shown in Fig. 3], but do not contribute to the visible-excited PL in the Raman region because of their lack of absorption of visible light, or because their emission bands lie entirely outside the carbon Raman region (2.18–2.28 eV in our experiments). Centers of the second type, which we have hypothesized to be sp^2-bonded carbon clusters, give rise to the visible-excited PL in the Raman region. Because of their low quantum efficiency, centers of the second type do not contribute directly to the observed CL, but do provide a competing nonradiative recombination channel that reduces the total CL intensity. Let N_1 be the number density of centers of the first type, and N_2 be the number density of centers of the second type. According to the above assumptions, an increase in the ratio N_2/N_1 will cause the total CL intensity to decrease, but will cause the intensity of the visible-excited PL to increase, explaining the observed inverse correlation.

A set of rate equations will now be derived for the luminescence kinetics of a system of two types of centers with the properties described. Model parameters for this system are defined as follows: Let N_1^* and N_2^* be the number densities of centers of types 1 and 2, respectively, in excited (luminescent) states. Let ν_1 and ν_2 be the total recombination rates of the two types of centers; the total recombination rate is defined as the sum of radiative (luminescence) and nonradiative recombination rates. Let η_1 and η_2 be the luminescence quantum efficiencies, i.e., the ratios of the radiative rate to the total recombination rate of each type of center. We have assumed that $\eta_1 \gg \eta_2$. In terms of the above parameters, the total luminescence intensity in either the CL or the PL experiment can be expressed as follows:

$$I_L = \eta_1 \nu_1 N_1^* + \eta_2 \nu_2 N_2^* \ . \tag{1}$$

In the PL experiment, let I_0 be the excitation photon flux, with dimensions $\mathrm{cm}^{-2}\,\mathrm{s}^{-1}$; let σ_1 and σ_2 be the optical-absorption cross sections of the two types of centers at the excitation photon energy (2.41 eV in our experiments). We have assumed that $\sigma_1 \ll \sigma_2$. The rate equations for the excitation of PL are then

$$\partial N_i^* / \partial t = I_0 \sigma_i N_i - \nu_i N_i \quad (i = 1,2) \ . \tag{2}$$

Substituting the steady-state solutions of Eq. (2) into Eq. (1), we obtain the steady-state PL intensity:

$$I_{\mathrm{PL}} = (\eta_1 \sigma_1 N_1 + \eta_2 \sigma_2 N_2) I_0 \ . \tag{3}$$

Assume that the small absorption cross section of the type-1 centers, rather than the small quantum efficiency of the type-2 centers, determines which term in Eq. (3) is smaller:

$$\eta_1 \sigma_1 N_1 \ll \eta_2 \sigma_2 N_2, \quad I_{\mathrm{PL}} \approx \eta_2 \sigma_2 N_2 I_0 \ . \tag{4}$$

The visible-excited PL then arises primarily from the type-2 centers, as observed.

In the CL experiment, let G_{eh} be the rate per unit volume (with dimensions $\mathrm{cm}^{-3}\,\mathrm{s}^{-1}$) for the generation of electron-hole (e-h) pairs in diamond by the primary electron beam. The value of G_{eh} is determined by the electron energy and current density of the electron beam and by the electronic properties of diamond. Let N_{eh} be the density of e-h pairs. Assume for simplicity that the e-h pairs recombine only at type-1 and type-2 luminescence centers. Let b_1 and b_2 be the bimolecular rates (with dimensions $\mathrm{cm}^3\,\mathrm{s}^{-1}$) for excitation of the two types of centers by capture of e-h pairs. The equation for e-h pair generation is then

$$\partial N_{eh} / \partial t = G_{eh} - (b_1 N_1 + b_2 N_2) N_{eh} \ . \tag{5}$$

The equations for excitation of the two types of centers by e-h pairs are

$$\partial N_i^* / \partial t = b_i N_i N_{eh} - \nu_i N_i^* \quad (i = 1,2) \ . \tag{6}$$

The steady-state CL intensity is found by substituting the steady-state solutions to Eqs. (5) and (6) into Eq. (1):

$$I_{\mathrm{CL}} = [(\eta_1 b_1 N_1 + \eta_2 b_2 N_2)/(b_1 N_1 + b_2 N_2)] G_{eh} \ . \tag{7}$$

The difference between the functional form of I_{PL} in Eq. (3), and of I_{CL} in Eq. (7), is due to the differing excitation mechanisms for these two processes. The rate for the excitation of a particular type of center in PL is proportional to the density of that type of center [Eq. (1)]. On the other hand, the rate for the excitation of e-h pairs, the initial step in the excitation of CL, is independent of N_1 and N_2; the e-h pairs may then be captured by either type of center in a branching process [Eq. (5)]. Assume that the small value of η_2 determines which term in the numerator of Eq. (7) is smaller:

$$\eta_1 b_1 N_1 \gg \eta_2 b_2 N_2 \ , \qquad I_{\rm CL} \approx [\eta_1 b_1 N_1 / (b_1 N_1 + b_2 N_2)] G_{eh} \ . \tag{8}$$

The observed CL then arises primarily from the type-1 centers. Assume also that the second term in the denominator of Eq. (7) is comparable to or larger than the first term:

$$b_1 N_1 \lesssim b_2 N_2 \ . \tag{9}$$

An increase in the value of n_2 will then cause $I_{\rm CL}$ to decrease by a significant amount, as observed in Fig. 5.

The inequalities in Eqs. (4) and (8), and (9) can be combined:

$$\sigma_1 N_1 / \sigma_2 N_2 \ll \eta_2 / \eta_1 \ll b_1 N_1 / b_2 N_2 \lesssim 1 \ . \tag{10}$$

The absorption coefficient of the type-1 centers in the visible region must be extremely small for these inequalities to hold.

The dependence of $I_{\rm PL}$ and $I_{\rm CL}$ on N_1 and N_2 can be expressed as follows:

$$I_{\rm PL} \approx c_1 N_2 \ , \tag{4a}$$

$$I_{\rm CL} \approx c_2 N_1 / (b_1 N_1 + b_2 N_2) \ , \tag{8a}$$

where (c_1, c_2) are constants. The model predicts that $I_{\rm PL}$ is directly proportional to N_2. On the other hand, $I_{\rm CL}$ is inversely proportional to N_2, provided that $N_2 > b_1 N_1 / b_2$. The inverse correlation between $I_{\rm CL}$ and $I_{\rm PL}$ is thereby quantitatively explained as a result of specimen-to-specimen variation in the density of type-2 centers. Any specimen-to-specimen variation in the density of type-1 centers, however, causes $I_{\rm CL}$ to vary in a manner uncorrelated with N_2 [Eq. (8a)]. Figures 5(b) and 5(c) show that the inverse correlation holds better for component (e) of the CL, the broad 2.85-eV band, than for components (a), (b), and (c). The results of Fig. 5 thus suggest that the density of the 2.85-eV centers is more constant from specimen to specimen than the combined density of the centers that give rise to CL components (a), (b), and (c).

CONCLUSION

Photoluminescence (PL), cathodoluminescence (CL), and Raman spectra were taken of a set of 48 diamond specimens grown by either filament-assisted or microwave-plasma-assisted CVD, and one gem-quality natural diamond. For these specimens, the laser-excited PL spectra in and near the carbon Raman region (1100–1800 $\rm cm^{-1}$ from the 514.5-nm laser line, or 2.18–2.28 eV) are broad and featureless; CL spectra in the 1.5–3.5-eV range show several distinct components. The laser-excited PL is found to be correlated in intensity with the sp^2-bonded carbon Raman band and is therefore attributed to sp^2-bonded carbon clusters. The CL spectra consist of several distinct components, which are attributed to centers derived from point defects and impurities. The spectrally integrated CL intensity is found to vary from specimen to specimen approximately inversely with the intensity of the laser-excited PL. The inverse correlation is especially strong for one component of the CL, a 2.85-eV band which is tentatively attributed to deep donor-acceptor pairs or dislocation-related defects.

To explain the inverse correlation between the CL and PL, we hypothesize that the luminescence centers in the CVD diamond films can be classified into two general types with differing excitation and recombination properties. According to our model, centers of the first type are characterized by high luminescence quantum efficiency and very weak absorption of visible light; centers of the second type (the sp^2-bonded carbon clusters) are characterized by low luminescence quantum efficiency and strong absorption of visible light. Centers of the second type then give rise to the PL excited by visible light. Both types of centers provide recombination channels for the electron-hole pairs excited in CL. Because of their low luminescence quantum efficiency, however, centers of the second type do not give rise to observable CL, but instead cause a decrease in the total observed CL intensity. An increase in the number density of centers of the second type is then predicted to increase the visible-excited PL intensity but reduce the CL intensity.

[1]L. H. Robins, L. P. Cook, E. N. Farabaugh, and A. Feldman, Phys. Rev. B **39**, 13 367 (1989).
[2]A. T. Collins, M. Kamo, and Y. Sato, J. Phys. D **22**, 1402 (1989).
[3]J. Walker, Rep. Prog. Phys. **42**, 1605 (1979).
[4]D. S. Knight and W. B. White, J. Mater. Res. **4**, 385 (1989).
[5]L. H. Robins, E. N. Farabaugh, and A. Feldman, J. Mater. Res. **5**, 2456 (1990).
[6]L. H. Robins, L. P. Cook, E. N. Farabaugh, and A. Feldman, Proc. SPIE **1146**, 166 (1990).
[7]A. M. Zaitsev, V. S. Vavilov, and A. A. Gippius, Krat. Soob. Fiz. **10**, 21 (1981) [Sov. Phys.—Leb. Inst. Rep. **10**, 15 (1981)].
[8]A. T. Collins, M. Stanley, and G. S. Woods, J. Phys. D **20**, 969 (1987).
[9]A. T. Collins and S. C. Lawson, J. Phys. Condens. Matter **1**, 6929 (1989).
[10]V. S. Vavilov, A. A. Gippius, A. M. Zaitsev, B. V. Deryagin, B. V. Spitsyn, and A. E. Aleksenko, Fiz. Tekh. Poluprovodn. **14**, 1811 (1980) [Sov. Phys. Semicond. **14**, 1078 (1980)].
[11]N. Yamamoto, J. C. H. Spence, and D. Fathy, Philos. Mag. B **49**, 609 (1984).
[12]J. Robertson, Adv. Phys. **35**, 317 (1986).